First publ. in: Materials Science and Engineering / A, 173 (1993), 1-2, pp. 347-350

Dynamics of the solidification of laser-annealed Si thin films

J. Boneberg, J. Nedelcu, H. Bender and P. Leiderer
Fakultät Physik der Universität Konstanz, 7750 Konstanz (Germany)

Abstract

Nanosecond time-resolved reflectivity and transmission measurements are used for the observation of solidification phenomena, following incomplete or complete melting of thin Si films ($d = 125$ nm) by nanosecond laser pulses. Solidification is observed to proceed at the liquid–solid interface as long as the film is not melted completely. On complete melting of the film, nucleation in the liquid becomes important. Heat conduction into the quartz substrate rapidly cools the liquid, until after several tens of nanoseconds homogeneous nucleation of crystalline Si occurs at temperatures around 500 K below the melting point of Si. At even larger supercoolings our measurements indicate the transient formation of amorphous Si in addition to the formation of the crystalline phase.

1. Introduction

Phase transformations at large deviations from equilibrium have gained considerable attraction since the discovery of the unique properties of metallic glasses. Metallic glasses are formed at quench rates of about 10^6 K s^{-1} (depending on alloy). The melting of thin films on non-reactive substrates by pulsed laser annealing allows the examination of nucleation and solidification phenomena at even higher quench rates: because of the large temperature gradients in the substrate the molten film can cool very rapidly ($\dot{T} > 10^{10}$ K s^{-1}). The supercooling before nucleation can reach $T_m/2$ [1]. In the following we use this experimental technique to study the dynamics of the solidification of thin Si films on a nanosecond time scale.

2. Experimental details

The samples used here were polycrystalline Si films (Sipos) with a thickness of 125 nm on a 1 mm quartz glass substrate. The annealing laser was a frequency-doubled Q-switched Nd:YAG laser with a pulse length of 7 ns (full width at half-maximum (FWHM)) and a beam profile close to TEM_{00}. The Nd:YAG pulse, incident nearly perpendicular to the surface (Fig. 1), was only mildly focused to a spot diameter of about 0.5 mm. For the measurement of the reflectivity we used two p-polarized continuous wave (CW) lasers: an He–Ne laser for the reflectivity from the surface ($\lambda = 633$ nm, 7 mW) with an angle of incidence of 45°, and an Ar laser for the reflectivity from the film–substrate interface. The angle of incidence onto the quartz glass was 35°. These two CW lasers were focused to a 1/e diameter of 12 μm on the surface and on the film–substrate interface respectively so that the variation in the pulse laser beam intensity across the diameter of the test laser foci could be neglected. The overlap of the two test laser foci was better than 90%. This was checked by a 1 μm pinhole in a 125 nm silver film on a quartz substrate of the same thickness. The specularly reflected or transmitted light was detected by pin diodes (risetime, less than 1 ns) and registered by a fast digital storage oscilloscope (HP54111D). Interference filters in front of the pin diodes suppressed contributions of the Nd:YAG light to the measured signal.

3. Results and discussion

The experimental results can be split into three regimes, depending on the energy density of the annealing laser: (i) heating of the solid without melting, (ii) partial melting and (iii) complete melting of the Si film. The temporal development of the reflectivities in these regimes is illustrated in Figs. 2–5.

3.1. Case (i)

As long as the energy density of the annealing laser pulse is sufficiently low ($E < E_m = 170$ mJ cm^{-2}) the film does not melt. Nevertheless, variations in the reflectivity are observed. In the experimental curves shown in Fig. 2 the energy density of the laser pulse is just below E_m. Both the reflectivity R_S of the film surface and the reflectivity R_i of the film–substrate interface decrease on heating by the laser radiation, R_S dropping from 70% to 30% and R_i from 50% to 40%. After the pulse both reflectivities relax back to the

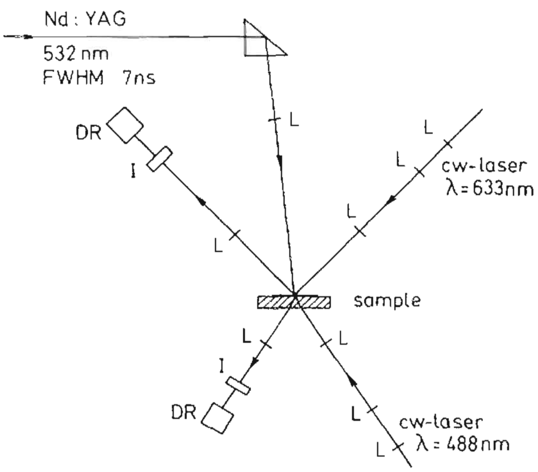

Fig. 1. Schematic set-up of the experiment: I, interference filter; L, lens; DR, pin diode for reflection measurements.

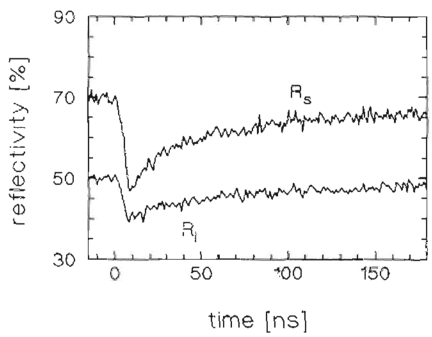

Fig. 2. $R(t)$ at a laser energy density of 160 mJ cm^{-2}: R_S, reflectivity at the surface; R_i, reflectivity at the film–substrate interface.

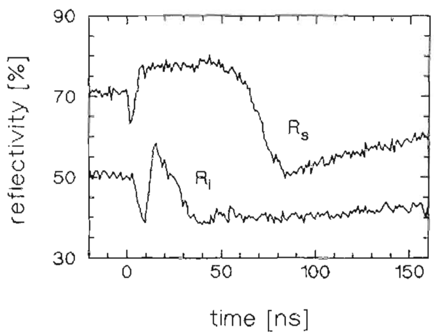

Fig. 3. $R(t)$ at a laser energy density of 240 mJ cm^{-2}.

starting value on a time scale of 200 ns. The observed reflectivity changes can be interpreted as arising from the temperature dependence of the optical constants of crystalline Si [2, 3]. Values calculated for R_S and R_i agree very well with the observed reflectivity changes.

3.2. Case (ii)

As the energy density is increased above E_m a surface layer of the Si film is melted and consequently additional structures in R_S and R_i appear (Fig. 3). The observed behaviour can be interpreted in the following way.

(1) The surface reflectivity R_S first drops with increasing temperature as for case (i). On melting, a rapid rise in R_S to the value for liquid Si occurs. As long as a liquid layer is present at the surface with a thickness $d_l > 2d_{ab}$ (d_{ab} absorption length in liquid Si, about 10 nm [4]) R_S remains nearly constant. Further thinning of the liquid layer below the penetration depth of light eventually leads to a decrease in R_S to the reflectivity of the hot solid Si near the melting point as shown in Section 3.1.

(2) The interfacial reflectivity R_i exhibits qualitatively the same behaviour; yet with some differences in detail. After the initial dip in R_S due to heating of the solid an increase is observed as the liquid–solid boundary approaches the substrate. The measured maximum in R_S, however, is smaller than expected for liquid Si, from which we conclude that in this case a thin layer of Si next to the glass substrate was not melted. The solidification proceeds from the unmelted Si layer towards the surface and R_i decreases once again towards the value for the hot solid Si at the melting point.

3.3. Case (iii)

On complete melting of the Si film the solidification scenario changes from the heterogeneous nucleation at the liquid–solid interface as in case (ii) towards homogeneous nucleation in the supercooled liquid. Therefore the reflectivity curves (Fig. 4) exhibit a behaviour different to that of Fig. 3. This behaviour can be explained in the following model as suggested by Stiffler *et al.* [5]. During the first plateau the liquid Si cools to a temperature several hundred kelvin below the melting point. Homogeneous nucleation then initiates solidification, which leads to a decrease in reflectivity. (Homogeneous nucleation is strongly supported by a transmission electron microscopy cross-sectional examination of the samples after irradiation, which reveals a nearly homogeneous distribution of nucleation sites [5].) The latent heat released on solidification raises the temperature towards the melting point, where further solidification is stopped. The layer consists now of Si crystallites in a liquid matrix and therefore has a reflectivity which is smaller than the reflectivity of liquid Si alone. The complete crystallization proceeds subsequently from the substrate towards the surface. Thus R_S has a second plateau which ends as the complete solidification reaches the surface layer.

In contrast to another measurement on thicker films [5], the homogeneous nucleation in our samples does not take place simultaneously across the whole film, as a comparison of $R_S(t)$ and $R_i(t)$ indicates: the steep decrease in R_i occurs about 25 ns earlier than the decrease in R_S. One can therefore conclude that owing to a thermal gradient in the film the homogeneous nucleation and solidification proceed from the substrate towards the surface. A comparison with data obtained by Stiffler [6] yields a supercooling of around 500 K for the example shown in Fig. 4.

Finally, we would like to discuss the behaviour at even higher supercoolings as displayed in Fig. 5 for a sequence of pulses at different energy densities. (It should be mentioned that the gradient-limited heat flux into the substrate leads to an increase in the quench rate, and therefore in the supercooling, as the energy density of the laser pulse is reduced. Thus somewhat surprisingly the largest supercooling is reached for the smallest energy density which is sufficient to melt the film completely.) An additional dip arises in the R_i curves for increasing supercooling. We interpret this dip as a signature of the transient formation of amorphous Si.

For thermodynamic reasons the nucleation of both crystalline and amorphous Si is possible if the supercooling is large enough [5]. Since the solidification of part of the liquid raises the film temperature, the amorphous portion will melt as the temperature T increases above $T_{m,a} = T_m - 225$ K [7] (where $T_m = 1685$ K and $T_{m,a}$ are the melting temperature of crystalline Si and amorphous Si respectively) and only the crystalline phase will survive. The eventual solidification process will therefore result in a polycrystalline film. The optical properties of the Si layer at room temperature after the annealing do not exchibit a change which could be attributed to the permanent formation of amorphous Si, as indicated by reflection and transmission measurements. Only at even higher quench rates, as they are obtained in thinner films, has permanent amorphization been observed by Sameshima and Usui [8].

Similar to the R_i curves in Fig. 5 the R_S curves (not shown here) indicate the effect of remelting as well, but in a slightly modified form: the remelting does not continuously increase with the supercooling. We suppose that the latent heat released on nucleation on the substrate side alters the nucleation on the surface side which always takes place some tens of nanoseconds later.

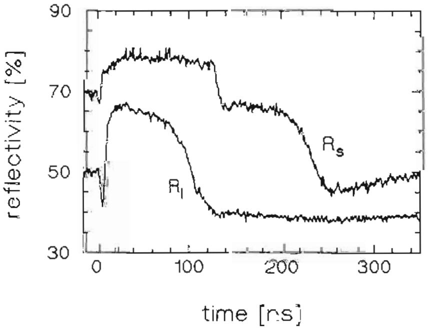

Fig. 4. $R(t)$ at a laser energy density of 363 mJ cm^{-2}.

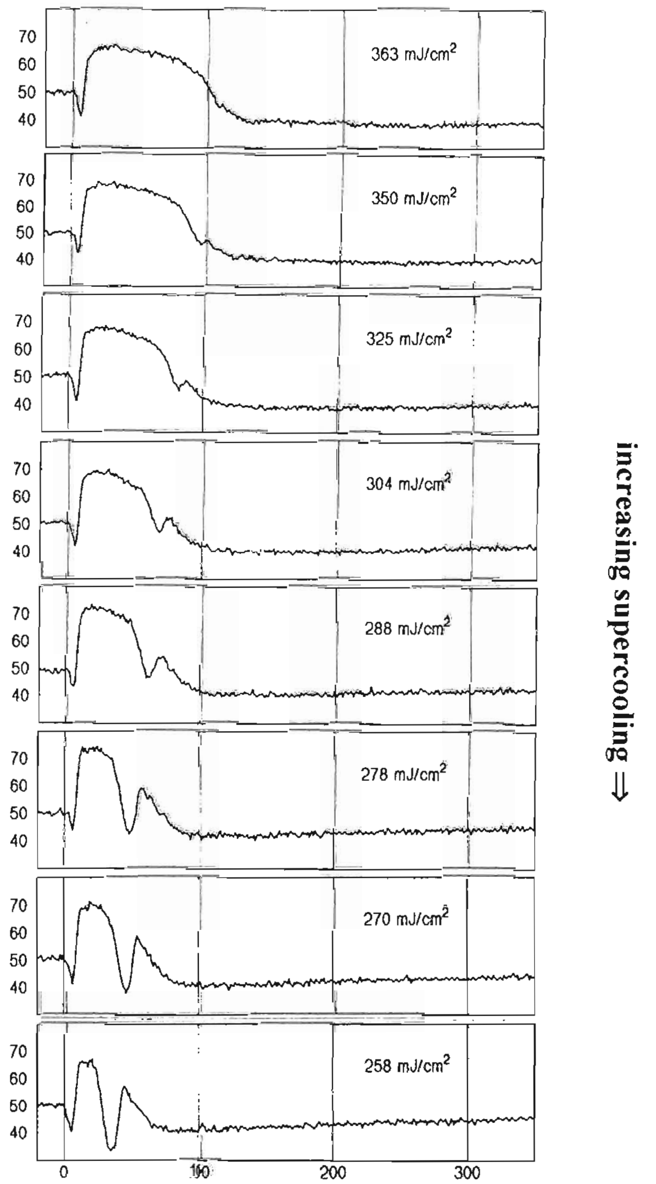

Fig. 5. $R_i(t)$ at various laser energy densities E. The supercooling increases with decreasing E (see ref. 6).

4. Conclusion

In summary we have shown that the simultaneous determination of the reflectivity measured at the surface and the film–substrate interface yields extensive information about nucleation and solidification in thin films. For the first time transient amorphization and the influence of the temperature gradient across the film on the nucleation process could be resolved.

Acknowledgments

This work was supported by Zentrum II für Energieforschung at the University of Konstanz.

References

1 S. R. Stiffler, M. O. Thompson and P. S. Peercy, *Phys. Rev. B, 43* (1991) 9851.
2 K. Murakami, K. Takita and K. Masuda, *Jpn. J. Appl. Phys., 20* (1981) L867.
3 G. E. Jellison and F. A. Modine, *Appl. Phys. Lett., 41* (1982) 180.
4 G. E. Jellison and D. H. Lowndes, *Appl. Phys. Lett., 51* (1987) 352.
5 S. R. Stiffler, M. O. Thompson and P. S. Peercy, *Phys. Rev. Lett., 60* (1988) 2519.
6 S. R. Stiffler, *Dissertation*, Cornell University, 1988.
7 E. P. Donovan, F. Spaepen, D. Turnbull, J. M. Poate and D. C. Jacobsen, *J. Appl. Phys., 57* (1985) 1795.
8 T. Sameshima and S. Usui, *J. Appl. Phys., 70* (1991) 1281.